

## Distribution of Low-Lying Quadrupole Phonon Strength in Nuclei

N. Pietralla,<sup>1</sup> P. von Brentano,<sup>1</sup> R. F. Casten,<sup>1,2</sup> T. Otsuka,<sup>3</sup> and N. V. Zamfir<sup>2,4,5</sup>

<sup>1</sup>*Institut für Kernphysik, Universität zu Köln, D-50937 Köln, Germany*

<sup>2</sup>*Brookhaven National Laboratory, Upton, New York 11973*

<sup>3</sup>*Department of Physics, University of Tokyo, Hongo, Bunkyo-ku, Tokyo 113, Japan*

<sup>4</sup>*Clark University, Worcester, Massachusetts 01610*

<sup>5</sup>*Institute of Atomic Physics, Bucharest-Magurele, Romania*

(Received 29 April 1994)

The distribution of quadrupole phonon strength to low-lying states in nuclei is examined. It is found that the  $2_1^+$  and  $4_1^+$  states of all nuclei from  $Z = 30$  to  $100$  display almost perfect quadrupole phonon character even though they encompass widely ranging structures. The interacting boson approximation reproduces both the very small deviations from phonon purity and the distribution of those deviations as a function of mean field structure in a natural fashion. Simple physical mechanisms explain these results.

PACS numbers: 21.10.Re, 21.60.Ev, 21.60.Fw

There has recently been renewed interest in the applicability of phonon models [1] in nuclear structure. Examples of phonon and multiphonon behavior have been found [2–10] in a variety of contexts ranging from spherical to transitional and deformed nuclei and from yrast states to intrinsic collective modes. The growing recognition that phonon modes are widespread, and that multiphonon excitations often survive intact in the low degeneracy nuclear environment, motivates a further study of the empirical and theoretical phonon structure and interrelationships of the low-lying yrast levels of collective nuclei. In particular, it was shown in Ref. [4] that an anharmonic vibrator, with constant anharmonicity, can describe the yrast energies of all nonrotational collective nuclei from  $Z = 30$  to  $82$ . It is therefore pertinent to ask if it is possible to directly test this phonon picture, that is, to assess whether or not the wave functions of the low-lying levels of collective even-even nuclei can be accurately described in terms of phonon excitations.

It is therefore the purpose of this Letter to use  $B(E2)$  values to show that the  $2_1^+$  and  $4_1^+$  levels for all nuclei from  $Z = 30$  to  $100$  display excellent quadrupole phonon purity and that this result is a natural property of the interacting boson approximation (IBA).

A quadrupole phonon excitation  $|2_1^+ 2\rangle$  of the ground state is defined by

$$|2_1^+ 2\rangle_{\text{ph}} \equiv N Q_{22} |0_1^+\rangle, \quad (1)$$

where  $Q_{22}$  is the quadrupole operator,  $N$  is a normalization factor, and the labels refer to spin, parity, and magnetic substate. Multiple “ $Q$ -phonon” states are created by repeated application of  $Q$ . Note that such states can be called phonons even for rotational excitations in that the phonon accelerates or decelerates the rotation.

This  $Q$ -phonon picture can be tested empirically or theoretically. If

$$B(E2:0_1^+ \rightarrow 2_i^+) = 0 \quad \text{for all } i > 1, \quad (2)$$

then Eq. (1) is satisfied for the  $2_1^+$  state. However, if the phonon strength is distributed over several  $2^+$  states, that is, if

$$|2^+ 2\rangle_{\text{ph}} = \beta_1 |2_1^+\rangle + \sum_{i>1} \beta_i |2_i^+\rangle, \quad \text{where } \sum_i \beta_i^2 = 1, \quad (3)$$

then Eq. (2) does not hold. A measure of the phonon distribution is given by

$$R^{(2)} \equiv \frac{\sum_{i>1} B(E2:0_1^+ \rightarrow 2_i^+)}{\sum_{i \geq 1} B(E2:0_1^+ \rightarrow 2_i^+)}. \quad (4)$$

where  $i$  labels the  $2^+$  states. From Eqs. (3) and (4), we have

$$R^{(2)} = \sum_{i>1} \beta_i^2 = 1 - \beta_1^2. \quad (5)$$

Thus,  $R^{(2)}$  directly measures the fraction of the  $Q$ -phonon strength to  $2_i^+$  levels *other* than  $2_1^+$  and indicates the 1-phonon purity of the  $2_1^+$  level. Of course, that collectivity may ultimately have origins in higher states such as the giant quadrupole resonance (GQR), but our purpose here is to focus on the *nature* of the resultant collectivity, not its microscopic *origins*, and on the phonon interrelationships of the low-lying yrast levels. Hence, in the sums in Eq. (4), it is necessary to explicitly exclude the GQR and to focus on the low-lying collective  $2^+$  states. In effect, we view Eqs. (1)–(5) as referring to the  $0\hbar\omega$  space, regardless of whether or not the microscopic origin of this collectivity resides in the GQR.

The same prescription for Eq. (4) arises from a complementary source. As the aim of the present study is to confront the data with calculations of collective nuclei, we need to choose a model that can offer predictions for a full variety of collective structures in a unified framework with a minimum of parameters. In practice, the only available model is the IBA [11], in which the full panoply of observed collective structures can be reproduced with only two parameters. (Ultimately, of course,

a shell model understanding of phonon structure would be desirable, but practical calculations for all mass regions and structural varieties are currently not feasible.) Inasmuch as the IBA is a valence space model for low-lying collective states, it is essential that the data set used in Eq. (4) do likewise.

First, we consider the experimental situation. We have evaluated empirical  $R^{(2)}$  values for all collective nuclei [nuclei with  $R_{4/2} = E(4_1^+)/E(2_1^+) > 1.9$ ] from Zn to Fm, where absolute  $B(E2)$  values to more than one  $2^+$  state are known. All known  $B(E2:0_1^+ \rightarrow 2_1^+)$  values to discrete  $2^+$  states were included. The results for 101 nuclei are summarized in Fig. 1. Though it is, of course, commonly recognized [12] that the  $B(E2)$  from the ground state to the  $2_1^+$  level is usually dominant, the *quantitative* degree of this dominance has not been discussed and is striking indeed.  $R^{(2)}$  is always small: it is  $<0.09$  in 96% of these nuclei (moreover three of the four exceptions have large errors).  $R^{(2)}$  is  $<0.06$  in 85% of the cases and its average value is about 0.03: Note that this overwhelming (97%) dominance and phonon purity is independent of the detailed structure of these nuclei, which comprise all varieties of structures including near harmonic and anharmonic vibrators,  $\gamma$ -soft nuclei, transitional nuclei, and rotors. The data in Fig. 1 also show interesting features in the *distribution* of  $R^{(2)}$  values, in particular, the peak near 8%–9%. This is *not* a statistical fluctuation but reflects a specific group of nuclei (Os) and type of structure: To see this, we show the  $R^{(2)}$  values for Hf–Pt in the inset to Fig. 1.

We now turn to the IBA. The  $2_1^+$  (and  $4_1^+$ ) states are pure phonon excitations in all three symmetries. Though long known for U(5), the phonon description of O(6) was only recently given [8].  $R^{(2)}$  vanishes for all three dynamical symmetries U(5), O(6), and SU(3), because the selection rules ( $\Delta n_d = 1$ ), ( $\Delta \tau = 1, \Delta \sigma = 0$ ), and

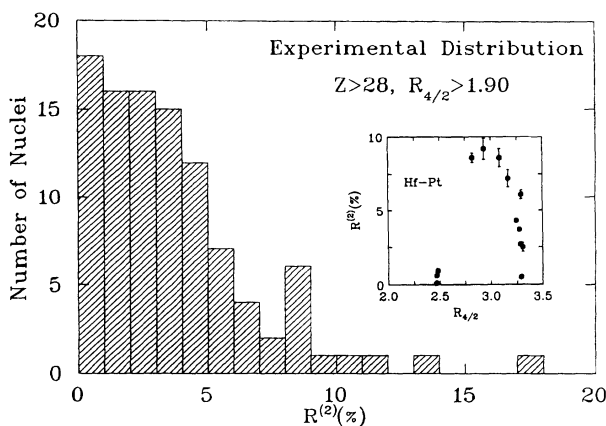


FIG. 1. Histogram of experimental  $R^{(2)}$  values for 101 nuclei from Zn to Fm obtained from all known  $B(E2:0_1^+ \rightarrow 2_1^+)$  values tabulated in the Nuclear Data Sheets. The inset shows detailed  $R^{(2)}$  values for Hf–Pt nuclei plotted against  $E(4_1^+)/E(2_1^+)$ .

$[\Delta(\lambda, \mu) = 0]$  forbid all  $E2$  transitions from the ground state to any state other than  $2_1^+$ . Outside the symmetries we study the behavior of  $R^{(2)}$  by systematically exploring the symmetry triangle (see Fig. 2) with the consistent  $Q$  formalism (CQF) [13], by writing

$$H = -\kappa Q(\chi) \cdot Q(\chi) + \epsilon n_d, \tag{6}$$

where

$$Q_{2\mu}(\chi) = s^\dagger d_\mu + d_\mu^\dagger s + \chi(d^\dagger d)_\mu^{(2)}. \tag{7}$$

The  $E2$  operator is  $T(E2) = e_B Q(\chi)$ . [The effective charge  $e_B$  cancels out in Eq. (4).] With no loss of generality, we take  $\kappa$  constant throughout at  $-0.025$  MeV.

We first study the U(5)  $\rightarrow$  O(6) transition leg which is the easiest to understand. In both limits we take  $\chi = 0$  and  $N = 6$ . The transition region is traversed by varying  $\epsilon$  (or, equivalently,  $\epsilon/\kappa$ ) from infinity [U(5)] to 0 [O(6)]. The results for  $R^{(2)}$  are shown in Fig. 2(a). The most striking feature is the extreme smallness of  $R^{(2)}$

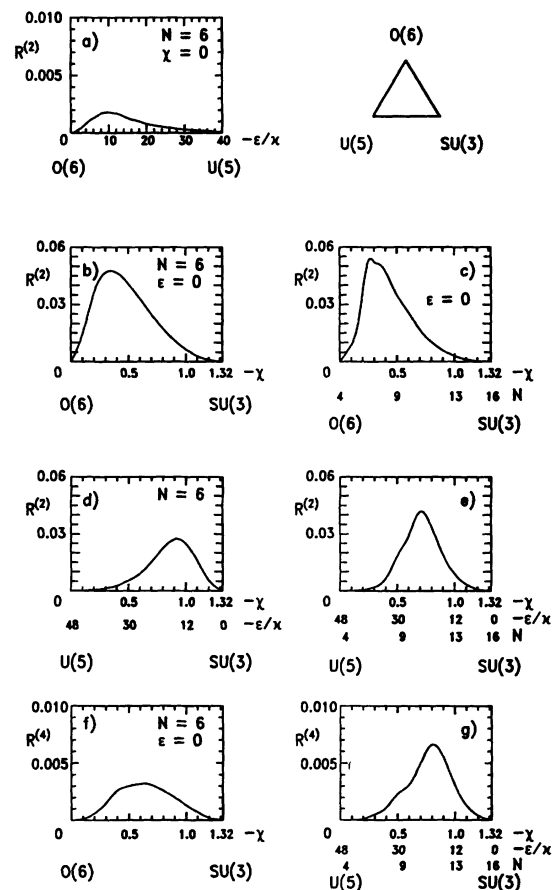


FIG. 2. Top right, the IBA symmetry triangle. The other panels give calculated values of  $R^{(2)}$  [or  $R^{(4)}$  for panels (f) and (g)] giving the absolute magnitude of phonon mixing in the  $2_1^+$  and  $4_1^+$  states in the IBA for various trajectories along the symmetry triangle. (See text for details.)

everywhere along the U(5)-O(6) transition:  $R_{\max}^{(2)}$  is only 0.002.

This result may be understood by expanding the IBA wave functions in an O(6) basis instead of the usual U(5) basis. The O(5) symmetry is common to both U(5) and O(6), and hence [14,15]  $\tau$  is a good quantum number throughout the transition from U(5)  $\rightarrow$  O(6), and the  $\Delta\tau = \pm 1$  selection rule for the  $E2$  operator also persists. Hence also the mixing of the  $0^+$  and  $2^+$  O(6) basis states is restricted to states with the same  $\tau$  and different  $\sigma$ . Except very close to U(5), then, the low-lying physical states are composed mostly of two O(6) components, with  $\sigma = N$  and  $N - 2$  [see Fig. 3(a)]. Contributions from O(6) basis states with  $\sigma < N - 4$  are only significant close to U(5). From the wave functions, the contribution of various  $E2$  matrix elements to the physical  $B(E2:0_1^+ \rightarrow 2_i^+)$  values can be quantitatively determined. There are only two significant nonvanishing contributions to  $B(E2:0_1^+ \rightarrow 2_i^+)$  values. For the  $B(E2:0_1^+ \rightarrow 2_1^+)$  value, the two O(6) amplitudes  $0^+(\sigma = N, \tau = 0) \rightarrow 2^+(\sigma = N, \tau = 1)$  and  $0^+(\sigma = N - 2, \tau = 0) \rightarrow 2^+(\sigma = N - 2, \tau = 1)$  add coherently while for the other [usually the  $B(E2:0_1^+ \rightarrow 2_3^+)$  value], by orthogonality, they nearly cancel. [The component  $0^+(\sigma = N - 4, \tau = 0) \rightarrow 2^+(\sigma = N - 4, \tau = 1)$  further enhances the cancellation as U(5) is approached.] Hence, the  $B(E2:0_1^+ \rightarrow 2_1^+)$  nearly exhausts the strength.

For O(6)  $\rightarrow$  SU(3),  $\varepsilon = 0$  and  $\chi$  varies from 0 to  $-1.32$ . Calculations were performed for  $N = 6$  and with  $N$  varying linearly with  $\chi$  from 4 to 16. The results in Figs. 2(b) and 2(c) show that  $R^{(2)}$  is again very small, with a maximum of  $\sim 0.05$ . A phonon description is thus again preserved to a very high degree. The U(5)  $\rightarrow$  SU(3) transitional region calculations were carried out by decreasing  $\varepsilon/\kappa$  as  $\chi$  varies in the range  $0 \rightarrow -1.32$ . As Figs. 2(d) and 2(e) show,  $R^{(2)} < 0.05$ .

These results can also be easily understood. It is again useful to use a different basis: We expand the wave functions in SU(3) [see Fig. 3(b)]. The primary mixing matrix elements, in this basis, have  $\Delta K = 0$  [15]. Thus

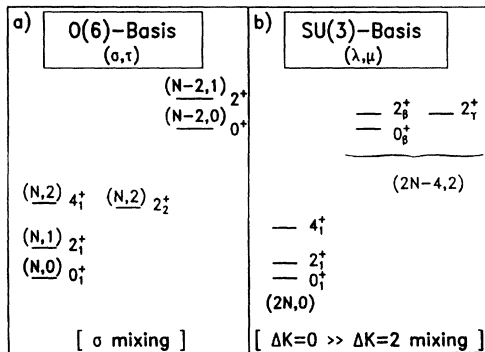


FIG. 3. Partial level schemes of O(6) and SU(3) showing the most relevant basis states.

the principal mixing for low-lying states is between the SU(3)  $K = 0$  ground band [( $2N, 0$ ) representation] and the  $K = 0$  ("beta") band of the [ $2N - 4, 2$ ] representation. However, the mixing of  $0^+$  and of  $2^+$  states is comparable, as are the intraband SU(3)  $E2$  matrix elements, and, hence, by orthogonality, the  $B(E2:0_1^+ \rightarrow 2_1^+)$  value is little affected by the mixing, and the  $B(E2:0_1^+ \rightarrow 2_\beta^+)$  value nearly vanishes by cancellation. However, there is also weak  $\Delta K = 2$  mixing of the SU(3)  $2_\gamma^+$  state (quasi- $\gamma$ -bandhead) with the  $2^+$  states of both the ground and the [ $2N - 4, 2$ ]  $K = 0$  excitations. Since there is no " $0_\gamma^+$ " level available to provide cancellation, both of these admixed  $2^+$  states contribute (the latter via the intermediary of the aforementioned  $\Delta K = 0$  mixing) to yield a small  $B(E2:0_1^+ \rightarrow 2_\gamma^+)$  value which is the main contributor to the numerator of  $R^{(2)}$ .

The results in Fig. 2 encourage us to pursue the validity of this  $Q$ -phonon picture in a more general context that comprises all the manifestations of collectivity in the IBA. We have therefore carried out a thorough set of calculations with a rather fine mesh of internal paths in the symmetry triangle. The results for  $N = 6$  are shown in the contour plot in Fig. 4. (Similar results are obtained for other  $N$  values.) Remarkably,  $R^{(2)}$  is *always* small. Its maximum values are along the O(6)  $\rightarrow$  SU(3) transition leg and, for any  $N \leq 16$ , the maximum value, independent of the IBA parameters (i.e., for any  $\kappa, \varepsilon, \chi$  in the symmetry triangle), is  $R^{(2)} < 0.07$ . The average value is  $\sim 0.02$ . As we saw in Fig. 1, the experimental values are equally small, averaging  $\sim 0.03$  and nearly always  $< 0.09$ . Thus, the IBA predicts that the  $2_1^+$  level is a nearly pure one-quadrupole-phonon excitation of the ground state induced by the  $0\hbar\omega$  operator  $Q$ . Note that this prediction is inherent to the model. Were the data different, the model predictions could not be altered accordingly.

The peak in  $R^{(2)}$  in Figs. 2 and 3 between O(6) and SU(3) is also interesting since it mirrors the empirical  $R^{(2)}$  distribution in the inset in Fig. 1. The maximum  $R^{(2)}$  values occur for precisely the nuclei  $^{186-192}\text{Os}$  that are the archetypical representatives of the O(6)  $\rightarrow$  rotor transition [16]. Thus, not only does the IBA reproduce the

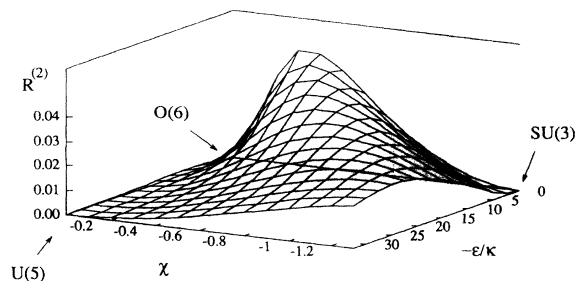


FIG. 4. Contour plot of  $R^{(2)}$  throughout the symmetry triangle.  $N = 6$ .

empirical fact of very small  $R^{(2)}$  values, but it reproduces the detailed distribution of  $R^{(2)}$  values across transition regions, as exemplified in Fig. 1 (inset).

It is useful to put these results in a more general context. The usual fermion  $E2$  operator consists of proton and neutron parts, with separate effective charges. This feature is conveyed to the boson situation in the IBM-2 (Ref. [17]), where

$$T(E2) = e_p^B Q_p^B + e_n^B Q_n^B. \quad (8)$$

In low-lying states, the proton and neutron motions are coherent, and such states are connected to the ground state predominantly by the isoscalar component of  $T$ . There is an overwhelming concentration of strength due to this operator from the ground state, leading to the  $Q$ -phonon picture. In this sense, the  $Q$  phonon is largely of isoscalar nature ( $F$  scalar for bosons), and the quadrupole-quadrupole interaction naturally favors this excitation at lower energy. At higher energies, there should be states excited by the isovector  $E2$  operator. In the IBM-2, these are mixed-symmetry states but are excited very weakly by  $E2$  transitions [18] [with  $B(E2:0_1^+ \rightarrow 2) \sim 10^{-1}-10^{-2}$  of  $B(E2:0_1^+ \rightarrow 2_1^+)$ ].

The above IBA analysis can be extended to the  $4_1^+$  state. As for the  $2_1^+$  state, we ask the extent to which  $|4_1^+ 4\rangle = N Q_{22} |2_1^+ 2\rangle$ : that is, we write

$$N Q_{22} |2_1^+ 2\rangle = \alpha_1 |4_1^+ 4\rangle + \sum_{i>1} \alpha_i |4_i^+ 4\rangle. \quad (9)$$

We define  $R^{(4)}$  analogously to Eq. (4) in terms of  $B(E2: 2_1^+ \rightarrow 4_1^+)$  values. Examples of the results are shown in Figs. 2(f) and 2(g):  $R^{(4)}$  is again very small. The maximum value for any  $N, \kappa, \epsilon$ , or  $\chi$  is only 0.01, which is nearly an order of magnitude less than  $R_{\max}^{(2)}$ . The reason is simple and interesting. As with  $R^{(2)}$ , the largest  $R^{(4)}$  values occur between O(6) and SU(3) and mixing arguments given for  $R^{(2)}$  apply here *except* that even the  $\gamma \rightarrow g$   $E2$  contribution to  $R^{(4)}$  is now largely cancelled since there are *both*  $2_\gamma^+$  and  $4_\gamma^+$  levels to mix with  $2_g^+$  and  $4_g^+$ . Note that the high purity of the  $4^+$  state holds for the  $Q_{22} |2_1^+ 2\rangle$  configuration:  $Q_{22} Q_{22} |0\rangle$  is less pure.

The above discussions highlight an important point. The small values of  $R^{(2)}$  and  $R^{(4)}$  are not somehow a trivial result but rather stem from basic properties of the symmetry limits, from the characteristic ways in which these symmetries are broken, and from subtle but pervasive and strong cancellation mechanisms.

To conclude, we have shown quantitatively that the empirical  $2_1^+$  states of all collective even nuclei from  $Z = 30$  to 100 nearly exhaust the known  $0\hbar\omega$   $E2$  strength from the ground state. Strength to all other known  $2^+$  states averages only about 3% and exceeds a 10% fraction in

only 1%–2% of nuclei (and most of these cases have large uncertainties). A thorough mesh of IBA calculations, comprising essentially all types of collective structures, shows that the model naturally and unavoidably produces exactly the empirical result:  $R^{(2)}$  is always less than 0.07 independent of the CQF-IBA Hamiltonian parameters. The agreement of calculated with empirical  $R^{(2)}$  values is not limited to global averages. For example, the large  $R^{(2)}$  values between Hf and Pt (Fig. 1, inset) are reproduced by the IBA for nuclei spanning an O(6)  $\rightarrow$  rotor region [Fig. 2(c), Fig. 4]. Finally, an even higher  $Q$ -phonon purity is calculated for the  $4_1^+$  state as a single  $Q$ -phonon excitation of the  $2_1^+$  state.

We thank Professor A. Gelberg for stimulating discussions. This work was supported in part under BMFT Contract No. 06OK602I, U.S. DOE Contracts No. DE-AC02-76CH0016 and No. DE-FG02-88ER40417, by the International Joint Research Projects of the Japan Society for the Promotion of Science, and by the DFG under the DFG-JSPS cooperation agreement.

- 
- [1] A. Bohr and B. Mottelson, *Nuclear Structure* (Benjamin, New York, 1975), Vol. II, and references therein.
  - [2] U. Kneissl *et al.*, Phys. Rev. Lett. **71**, 2180 (1993); A. Zilges *et al.*, Phys. Rev. Lett. **70**, 2880 (1993).
  - [3] M. Deleze *et al.*, Nucl. Phys. **A551**, 269 (1993); R. F. Casten *et al.*, Phys. Lett. B **297**, 19 (1992).
  - [4] R. F. Casten, N. V. Zamfir, and D. S. Brenner, Phys. Rev. Lett. **71**, 227 (1993).
  - [5] X. Wu, A. Aprahamian, J. Cato-Ceron, and C. Baktash, Phys. Lett. B **316**, 235 (1993).
  - [6] H. G. Börner *et al.*, Phys. Rev. Lett. **66**, 691 (1991).
  - [7] P. von Brentano *et al.*, Nucl. Phys. **A557**, 593c (1993).
  - [8] G. Siems *et al.*, Phys. Lett. B **320**, 1 (1994).
  - [9] W. Korten *et al.*, Phys. Lett. B **317**, 19 (1993).
  - [10] A. Zilges *et al.*, Z. Phys. A **340**, 155 (1991).
  - [11] A. Arima and F. Iachello, *The Interacting Boson Model* (Cambridge University Press, Cambridge, 1987); Phys. Rev. Lett. **35**, 1069 (1975).
  - [12] W. Andrejtscheff and P. Petkov, Phys. Rev. C **48**, 2531 (1993).
  - [13] D. D. Warner and R. F. Casten, Phys. Rev. Lett. **48**, 1385 (1982).
  - [14] A. Leviatan, A. Novoselsky, and I. Talmi, Phys. Lett. B **172**, 144 (1986).
  - [15] R. F. Casten and D. D. Warner, Phys. Rev. Lett. **48**, 666 (1982); Rev. Mod. Phys. **60**, 389 (1988).
  - [16] R. F. Casten and J. A. Cizewski, Nucl. Phys. **A309**, 477 (1978).
  - [17] A. Arima, T. Otsuka, F. Iachello, and I. Talmi, Phys. Lett. **66B**, 205 (1977).
  - [18] B. Fazekas *et al.*, Nucl. Phys. **A548**, 249 (1992).